ELSEVIER

Journal of Chromatography A, 916 (2001) 191–200

JOURNAL OF CHROMATOGRAPHY A

www.elsevier.com/locate/chroma

Discrete spacers for photometric characterization of humic acids separated by capillary isotachophoresis

Iveta Nagyová[a], Dušan Kaniansky[b,*]

[a]*Department of Chemistry, Faculty of Natural Sciences, Matej Bel University, Tajovského 40, SK-974 01 Banská Bystrica, Slovak Republic*

[b]*Department of Analytical Chemistry, Faculty of Natural Sciences, Comenius University, Mlynská Dolina CH-2, SK-842 15 Bratislava, Slovak Republic*

Abstract

A group of twenty discrete spacers suitable for photometric characterization of humic acids (HAs) after their isotachophoretic (ITP) separation at pH 10 was found. The spacers, inorganic and organic acids and amino acids of suitable acid–base and migration properties exhibiting no light absorption in the UV region of the light spectrum, made possible to perform this characterization in a sensitive spike mode of the ITP analysis. Using this approach a complex mixture of humic constituents present in a test HA preparation was separated into 22 fractions migrating in the interzonal boundary layers formed by the zones of discrete spacers and 21 fractions mixed with the zones of the spacers. A photometric monitoring of the fractions in the ITP stack at a 405 nm detection wavelength provided an adequate selectivity and sensitivity into the characterization. Relative sizes of the detected fractions of the test HA preparation ranged from 0.2–0.3 to 27.5% (based on the response of the phototometric detector at 405 nm). The fractions representing ca. 0.2–0.3% of the total peak area could be still quantified when 800 ng of the test preparation was loaded onto the ITP column. A typical repeatability of the total area of the detection signal corresponding to humic constituents in the ITP stack was ca. 2.5%. Repeatabilities of the peak areas of the fractions of the humic constituents defined by the spacers ranged from 2 to 6% for the fractions representing 1% or more of the total area and from 8 to 12% for those representing less than 1%. No marks of aggregations of the humic constituents were detected and reproducible ITP profiles (fingerprints) of the studied humic preparation were achieved under the developed working conditions.

Keywords: Isotachophoresis; Photometric detection; Detection, electrophoresis; Humic acids; Fulvic acids; Humic substances

1. Introduction

Humic substances (HSs) constitute bulk of soil organic matter and they are characterized as amorphous, dark-coloured, partly aromatic, mainly hydrophilic, chemically complex, polyelectrolyte-like materials which range in molecular mass from a few hundred to several thousand [1]. Based on differences in the solubilities in alkali and acid, HSs form three main fractions [1–6]: (1) humic acids (HAs; the fraction of HS soluble in dilute alkali but coagulating on acidification of the alkaline extract); (2) fulvic acids (FAs; the fraction of HS soluble in both dilute alkali and dilute acid); (3) humin (the fraction of HSs which cannot be extracted from soil samples by dilute base or acid).

Analytical characterisations of HSs isolated from

*Corresponding author. Fax: +42-1765-425-360.

E-mail address: kaniansky@fns.uniba.sk (D. Kaniansky).

0021-9673/01/$ – see front matter
PII: S0021-9673(00)01095-5

soil or water by suitable extraction procedures [1–8] have a practical relevance, e.g. in agriculture, ecology, water processing and storage of waste. The ionogenic nature of HAs and FAs present in HS samples makes capillary electrophoresis (CE) separation techniques analytical alternatives to such characterizations [9–35]. In addition, CE techniques are useful in investigations of complexations of HSs with metal cations [9,12,15,16,25,28], in estimations of HA contents in soils [24] and in studies investigating decompositions of HAs [23,34]. So far all CE techniques were employed to the separations of HAs and FAs. In this context we should mention the use of capillary isotachophoresis (ITP) [9,10], capillary zone electrophoresis (CZE) in free solutions [11–21,23–28] and in cross-linked [18,23] and replaceable [35] gels, micellar electrokinetic chromatography (MEKC) [18] and capillary isoelectric focusing (cIEF) [22].

In dependence on pH and the ionic strength FAs and, mainly, HAs tend to aggregate in aqueous solutions [1]. The aggregates can be kinetically stable and/or entities slowly decomposing during the CE separation. They have a clear impact on the electrophoretic profiles of HS samples as provided, for example, by CZE [26,33]. Changes in the CZE profiles of HAs and FAs may also originate in their interactions with the carrier electrolyte constituents. For example, borate present in the carrier electrolyte solution was shown to significantly influence the profile [20,21,26,29,30,33] and boric acid was demonstrated to provide up to 30 fractions of humic constituents [30]. Influences of organic modifiers present in the carrier electrolyte solutions on the CZE fingerprinting of HAs and FAs were also documented [17]. Interactions of some humic constituents with polyvinylpyrrolidone added to the ITP electrolyte system were shown to have dramatic impacts on their effective mobilities [10]. Recent chromatography results by Tonelli et al. [36] shows that also pyrophosphate (currently used in the isolation of HAs from soil) can participate in the formation of stable entities with some HAs. These facts indicate that in the CE characterizations (fingerprinting) of HSs both the mutual associations of the HA and FA constituents (aggregations) and interactions of these constituents with the electrolyte components in which the separations are performed may adversely affect the characterization (fingerprinting). While the latter disturbances can be eliminated via the use of an appropriately chosen electrolyte system a suitable sample preparation step may become essential to eliminate negative impacts of the associations of the humic constituents on the electrophoretic profiles.

The ITP separation is accompanied by a selfsharpening effect due to a stepwise course of the electric field strength along the ITP stack [37,38]. This effect, restoring the ITP steady state along the stack, in fact, continuously eliminates negative impacts of dispersive phenomena on the profiles of the zones. For example, in the separations of complexes of metals it eliminates zone dispersions due to (slow) decompositions of the complex particles during their ITP migration [39]. In this context it is logical to assume that the selfsharpening effect acts analogously in the separations of HS samples when the decompositions of the aggregates, into which the HA and FA constituents can be bound [26,33], occur. These capabilities, offering in some respects a substitute for the sample preparation, and well defined concentrating properties of ITP [37,38] stimulated our interest in the use of this technique to characterization of HSs.

Considering multicomponent natures of HS samples and light absorption properties of their HA and FA constituents we favored the use of ITP in the spike mode of analysis [10,37,38,40–43] in a combination with photometric characterizations of the resolved fractions. Promising possibilities of this approach demonstrated also our previous results dealing with the ITP characterizations of HS based on the interactions of the HSs constituents with polyvinylpyrrolidone at a low pH [10]. From the quoted works it is apparent that analytical advantages of the spike mode are closely linked with the formations of large numbers of the interzonal boundary layers (migration positions of the analytes), e.g. by the zones of discrete spacers, and the use of selective detection. Therefore, the choice of a multicomponent group of constituents suitable for spacing HA and FA constituents and compatible with the UV photometric detection was an essential task of this work. Quantitative aspects of the characterizations of HA and FA fractions provided by the ITP separation of a test HS preparation in the presence of an

optimum mixture of the discrete spacers were assessed in this context. Although no marks of aggregations of HAs and FAs were detected in the ITP separations at a low pH [9,10], this cannot be excluded in general [1–6], and the separations at a high pH were preferred in this work.

2. Experimental

2.1. Instrumentation

A prototype of an ITAChrom EA 101 capillary electrophoresis analyzer (J & M, Aalen, Germany) was used in our experiments. It was assembled with the column-coupling configuration of the separation unit using modules supplied by the manufacturer. The preseparation column was provided with a 800 μm I.D. capillary tube made of fluorinated ethylene–propylene (FEP) copolymer. The length of the capillary tube was 90 mm. A 300 μm I.D. capillary tube made of FEP (160 mm in the length) was used in the analytical column. The driving currents were 200 and 40 μA in the preseparation and analytical columns, respectively. The sample solutions were injected into the analyzer with the aid of a 701 N microsyringe (Hamilton, Bonaduz, Switzerland) into a 30 μl loop of the injection valve filled either with water or aqueous solutions of the discrete spacers.

2.2. Chemicals, samples and electrolyte solutions

The leading and terminating electrolyte solutions were prepared from chemicals obtained from Serva (Heidelberg, Germany), Sigma (St. Louis, MO, USA), Merck (Darmstadt, Germany) and Lachema (Brno, Czech Republic). Hydroxyethylcellulose 4000 (HEC) served as an electrooosmotic flow suppressor in the leading electrolyte solution. Its 1% (w/v) aqueous solution was purified on a mixed-bed ion-exchanger (Amberlite MB-1, Serva). Water obtained by a Pro-PS purification system (Labconco, Kansas City, KS, USA) was used for the preparation of the electrolyte solutions.

Aqueous stock solutions of the discrete spacers used in this work (see below) were prepared from chemicals provided by the above suppliers.

Humic acid (HA preparation) with molecular mass in the range of 600–1000 was obtained from Fluka (Buchs, Switzerland; Catologue No.53 680). A stock solution of the acid (100 mg/l) was prepared by its dissolution in a 1 m*M* aqueous solution of Tris. The solution was sonicated for 1 min in a low power laboratory ultrasonic bath and filtered through a 1.2 μm pore size membrane filter (Sigma).

Absorption of CO_2 by the electrolyte solutions was prevented by keeping the solutions in closed vessels and permanently placed in a desiccator over NaOH pellets. The terminating electrolyte solution in the terminating electrode compartment of the analyzer was maintained in a closed environment using a gas proof cap. The ambient pressure above the solution in the compartment was preserved via a microcolumn packed with NaOH pellets. The microcolumn was tightly connected to the electrode compartment via a Luer female connector in the cap.

3. Results and discussion

The composition of the electrolyte system used in the ITP separations of the studied HA preparation is given in Table 1. This electrolyte system was chosen for our experiments for the following reasons: (1) Acidic groups of HAs and FAs are ionized completely (carboxylic) or to high degrees (phenolic) at pH 10 and, therefore, aggregations of these constituents should not be significant in the separations under such acid–base conditions [1]. (2) Its leading and terminating anions provided the widest possible span of the effective mobilities for the ITP migrations of the humic constituents at pH 10. This was due to the fact that chloride used as the leading anion is one of

Table 1
Electrolyte system

Parameter	
Solvent	Water
Leading anion	Chloride
Concentration (m*M*)	10
Counter ion	Ethanolamine
Suppressor of electroosmotic flow	HEC[a]
Concentration (%, w/v)	0.2
pH of the leading electrolyte	10.00
Terminating anion	OH^-(water)

[a] HEC = Hydroxyethylcellulose.

the most mobile anions at this pH while OH^- is the slowest terminating anion in the anionic ITP separations in aqueous electrolyte systems [38].

3.1. Discrete spacers for characterizations of HAs

Typical isotachopherograms as obtained from the separations of the constituents present in the studied HA preparation (see Experimental) by the photometric detector operating at a 254 nm detection wavelength (Fig. 1) show its heterogeneous nature. This is in a general agreement with the results of the CE separations of this HA preparation as reported previously [10,20–27,30,33]. Apparently, this heterogeneity as visualized by the isotachopherograms was enhanced by the zones of anionic constituents (''impurities'') originating from the leading and terminating electrolyte solutions [the zone of carbonate (1, in Fig. 1) and the zones of unidentified constituents a, b and c in Fig. 1]. The zones of these constituents, acting as discrete spacers [10,37,38,40–43], split a tight ITP stack of the HA constituents into 5 fractions (I–V, in Fig. 1) and, in fact, improved interpretabilities of the isotachopherograms. On the other hand, from the isotachopherogram in Fig. 1C (obtained in a blank ITP run) we can see that the electrolyte solutions contained also anionic constituents (''impurities'') absorbing UV light at 254 nm (v, w, x, y and z, in Fig. 1C). These impurities, migrating in the boundary layers between the zones of the UV light non-absorbing impurities (1, a, b and c, in Fig. 1), introduced (subtractable) systematic biases into the quantitations of the HA fractions (I–V, in Fig. 1).

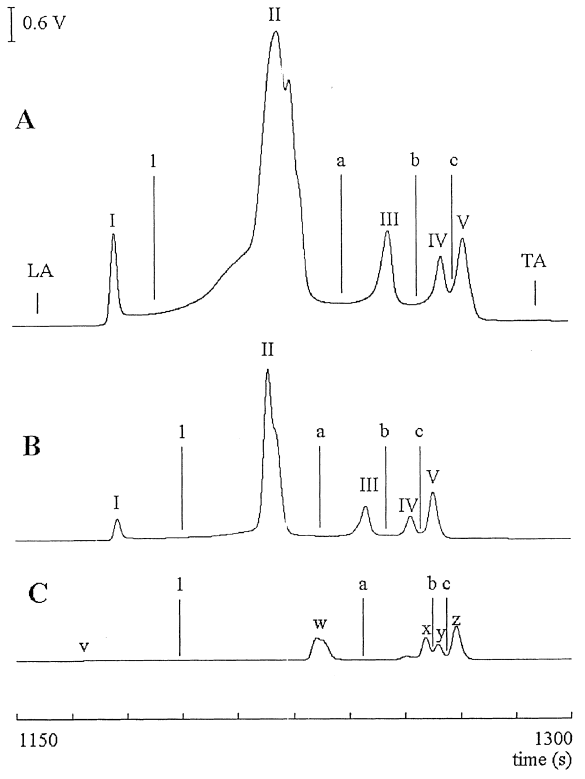

Fig. 1. Isotachopherograms obtained from the separations of HA constituents by the photometric detector (254 nm) in the analytical column. The records correspond to 800 ng (A) and 100 ng (B) loads of the HA preparation into the equipment. The record from the blank run (C) is given as a reference. The separations were performed in the electrolyte system described in Table 1 with 200 and 40 μA driving currents in the preseparation and analytical columns, respectively. I–V = HA fractions; 1 = carbonate; a, b and c = UV light non-absorbing anionic impurities originating from the electrolyte solutions; v, w, x, y and z = UV light absorbing anionic impurities originating from the electrolyte solutions. LA, TA = leading and terminating anions, respectively.

The isotachopherograms in Fig. 1 clearly imply that the separation of the HA preparation with a multicomponent mixture of discrete spacers compatible with the photometric detection should further enhance its fractionation. To find such a mixture of discrete spacers, we assessed ITP separabilities of 43 organic and inorganic acids and amino acids, exhibiting no light absorption at 254 nm. To keep such a search rational we employed combinations of computer predicted migration orders [44] of these constituents, based on the steady-state ITP model [37,38], with experimental evaluations of these predictions. A mixture of discrete spacers of the composition given in Table 2 was chosen as an optimum as it consisted of a maximum number of the constituents separable in one ITP run under the electrolyte conditions employed in this work (Table 1). In this context it is to be noted that the data in Table 2 show a good agreement of the predicted and experimentally found migration orders of the spacing constituents.

Isotachopherograms in Fig. 2 illustrate a significantly enhanced fractionation of the HA preparation attributable to the use of the mixture of discrete spacers chosen for our characterization. From the isotachopherograms it is visible that the HA con-

Table 2
Spacing constituents for photometric characterization of HA separated by ITP at pH 10, their pK values, absolute ionic mobilities and calculated parameters of their zones under the ITP steady state conditions

Migration order[a]		Spacing constituent	p$K_{A,1}$	p$K_{A,2}$	p$K_{A,3}$	$m_{o,1}$	$m_{o,2}$	pH[c]	$m_{eff.}$[c]
Exp	Predict								
1	1	Carbonic	6.35	10.33		46.1	71.8	10.09	55.4
2	–	ADA[b]	6.6	–		–	–	–	–
3	3	Aspartic	3.9	10.00		30.9[x]	55.4[x]	10.13	45.0
4	4	Glutamic	4.32	9.96		28.5[x]	53.0[x]	10.14	43.3
5	5	2-Aminoadipic	4.21	9.77		26.8[x]	44.0[x]	10.16	39.0
6	6	2-Aminopimelic	4.3[x]	9.8[x]		25.0[x]	44.0[x]	10.17	38.3
7	7	Taurine	8.89			35.0		10.20	33.4
8	–	Boric	9.24	12.74	13.8	–	–	–	–
9	9	Glycylglycine	8.24			31.9		10.21	31.6
10	10	Asparagine	8.79			30.1		10.24	29.1
11	11	MES[b]	6.18			28.3		10.24	28.3
12	13	Methioninesulphoxide	8.58			26.9		10.28	26.4
13	12	MOPSO[b]	6.95			26.6		10.27	26.6
14	14	DIPSO[b]	7.59			25.0		10.29	25.0
15	15	TAPSO[b]	7.67			24.0		10.31	23.9
16	16	AMPSO[b]	8.95			22.1		10.37	21.3
17	17	Citruline	9.53			24.2		10.39	21.3
18	18	Norleucine	9.71			23.8		10.43	20.0
19	19	β-alanine	10.24			29.2[x]		10.52	19.2
20	20	Proline	10.64			27.0[x]		10.79	15.7

[a] Experimentally obtained (Exp) and predicted (Predict) migration orders under the electrolyte conditions described in Table 1. pK_A and m_o values were taken from the literature [49–55] or they were estimated from the ITP separations (*) [44].

[b] ADA = *N*-(2-acetamido)iminodiacetic acid; MES = 2-(*N*-morpholino)ethanesulfonic acid; MOPSO = 3-(*N*-morpholino)-2-hydroxypropanesulfonic acid; DIPSO = 3-[*N*-bis(2-hydroxyethyl)amino]-2-hydroxypropanesulfonic acid; TAPSO = 3-[*N*-tris(hydroxymethyl)-methylamino]-2-hydroxypropa-nesulfonic acid; AMPSO = *N*-(1,1-dimethyl-2-hydroxyethyl)-3-amino-2-hydroxypropanesulfonic acid.

[c] pH, $m_{eff.}$ = calculated for the ITP steady state conditions [37,38].

stituents migrated either in the boundary layers between the pairs of the discrete spacers or in the mixed zones with the spacers. From general relationships relevant to the migration order of the ITP separands [38,45] it is apparent that a particular HA constituent, HA_i, migrated between the corresponding spacing constituents X (front spacer) and Y (rear spacer) when the following conditions were met:

$$\bar{m}_{HA_i,X_{mix}} < \bar{m}_{X,X_{mix}}$$

$$\bar{m}_{HA_i,Y_{mix}} > \bar{m}_{Y,Y_{mix}}$$

Here, $\bar{m}_{HA_i,X_{mix}}$ and $\bar{m}_{HA_i,Y_{mix}}$ are the effective mobilities of the ith HA constituent in the zones of discrete spacers X and Y, respectively, while $\bar{m}_{X,X_{mix}}$ and $\bar{m}_{Y,Y_{mix}}$ are symbols for the effective mobilities of discrete spacers in their own zones. The subscript *mix* indicates that the physico–chemical properties of this zone are determined besides X also by comigrating HA constituents. On the other hand, the jth HA constituent, HA_j, migrated in the zone of discrete spacer X when the following condition was met [38,45]:

$$\bar{m}_{HA_j,X_{mix}} = \bar{m}_{X,X_{mix}}$$

From these general equations and from isotachopherograms in Figs. 2 and 3 it is clear that the pH values in the zones of some spacers (more mobile than MES (11)) and their effective mobilities as given in Table 2 are to be considered only as certain approximations since they were calculated for pure ITP zones.

Considering a multicomponent nature of the HA preparation it is logical to assume that each of the 22 interzonal boundary layers [formed by the zones of

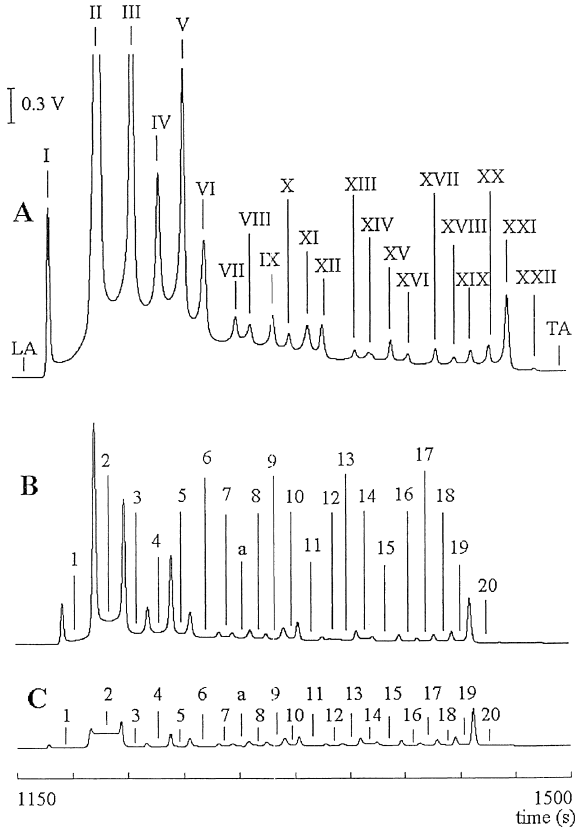

Fig. 2. Isotachopherograms obtained from the separations of HA constituents in the presence of discrete spacers by the photometric detector (254 nm) in the analytical column. The records correspond to 800 ng (A) and 100 ng (B) loads of the HA preparation into the equipment. The record from the run with the discrete spacers (C) serves as a reference. The concentrations of the discrete spacers in the injected sample (a 30 μl volume by the sample loop of the injection valve) were 50 μmol/l. I–XXII = fractions of HA; 1–20 = the zones of discrete spacers (the numbers correspond to those in Table 2, Exp); a = a UV light non-absorbing electrolyte impurity acting as a discrete spacer. LA, TA = leading and terminating anions, respectively.

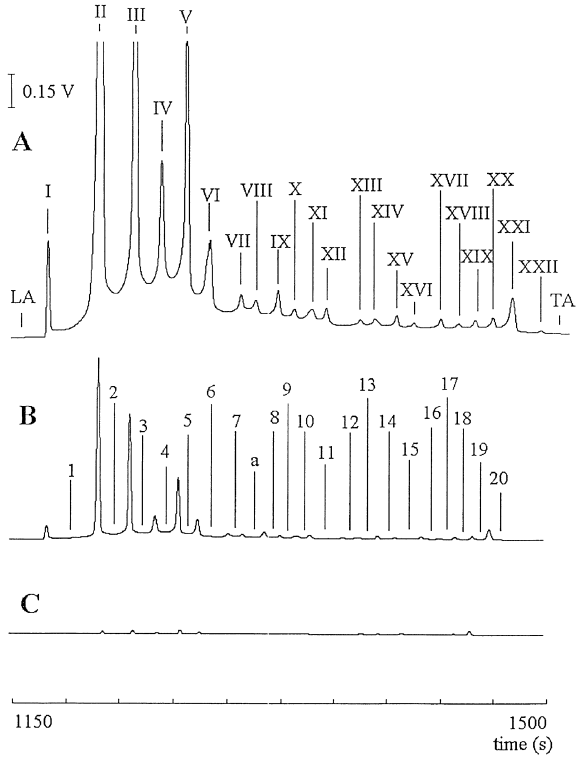

Fig. 3. Isotachopherograms from the separations of HA constituents under the same conditions as in Fig. 2 only the detection wavelength was set at 405 nm. The records correspond to 800 ng (A) and 100 ng (B) loads of the HA preparation into the equipment. The record from the run with the discrete spacers (C) serves as a reference. The concentrations of the discrete spacers in the injected sample (30 μl by the sample loop of the injection valve) were 50 μmol/l. The meaning of the symbols is the same as in Fig. 2. For the driving currents see Fig. 1.

20 discrete spacers (Table 2), the zone of the electrolyte impurity (a) and the zones of the leading and terminating anions; in this context we should note that the zones of impurities b and c (Fig. 1) formed in the presence of the mixture of discrete spacers mixed zones with MES and TAPSO, respectively] was occupied by more than one HA constituent. A shift of the baseline of the detection signal in the isotachopherogram visible, especially, in the runs with higher loads of the HA sample (see, e.g. Fig. 2A) indicates that the same applies for the HA constituents migrating in the mixed zones with the discrete spacers.

From the isotachopherograms in Figs. 2A and 2B we can see that the HA constituents were distributed, mainly, in the front part of the ITP stack. This indicates relatively high effective mobilities of the majority of the HA constituents of the test HS preparation. Approximate calculations revealed that more than 95% of the isotachophoretically migrating HA constituents had the effective mobilities higher than that of MES (11, in Fig. 2). Although the spacing constituents reduced absolute contributions of the UV light absorbing ''impurities'' (originating from the electrolyte solutions) to the peak sizes of

the HA fractions from the isotachopherograms in Figs. 1 and 2 we can see that, especially, in the rear part of the ITP stack (the peaks Nos. XIII–XXII) the contributions were still significant.

3.2. ITP–photometric characterization of HAs at a 405 nm detection wavelength

It was shown [9,10] that the photometric detection of HAs and FAs in ITP can be performed at a 405 nm wavelength. Our experiments carried out under such detection conditions (see Fig. 3) revealed reductions of disturbances due to the UV light absorbing ''impurities'' originating from the electrolyte solutions. Evaluations of the experimental data showed that ratios of the total areas of the peaks of the impurities at 254 and 405 nm (Figs. 2C and 3C) were approximately 13:1. On the other hand, the corresponding ratios of the total peak areas of the HA constituents at these detection wavelengths, under otherwise identical working conditions, were approximately 2:1 (Figs. 2A and 3A). In addition, mutual ratios of the peak areas of the HA fractions at the two wavelengths were practically constant with the exception of those with higher background signals at 254 nm (see, e.g. XXI in Figs. 2 and 3). These results clearly illustrate a benefit attributable to the use of the photometric detection of HAs at 405 nm under our separating conditions.

Blank runs with the discrete spacers (Fig. 4) were performed regularly in our experiments to assess the reproducibilities of the background in the migration positions of the HA fractions. Total areas of the background peaks agreed within less than 15% for different lots of the electrolyte solutions. These fluctuations corresponded to 0.15% of the total sizes of the peak areas for maximum injected amounts of the HA preparation (800 ng). Such small and reproducible background values undoubtedly contributed to reproducible profiles of the HA constituents in the ITP stack also in a long-term time frame (Fig. 5). Typical repeatabilities of the total areas of the detection signal for isotachophoretically migrating HA constituents and repeatabilities of the peak areas for the HA fractions (peaks) are summarized in Table 3.

The calibration curve (the total area of the signal from the photometric detector at 405 nm corresponding to the HA constituents) was determined for 50–800 ng loads of the HA preparation. It was described by a linear regression equation: $A = 1453 + 70\,256M$ (A = peak area in mVs units; M = the amount of HAs in μg) with a correlation coefficient of 0.9970 for 15 data points. Such a course of the calibration curve implies the presence of identical species in the ITP stack for various sample loads (in the case of significant formations of concentration dependent aggregates by the HA constituents one would expect the presence of the species differing in the light absorptivities and in the effective mobilities relative to those existing at low concentrations of HAs [26,33]).

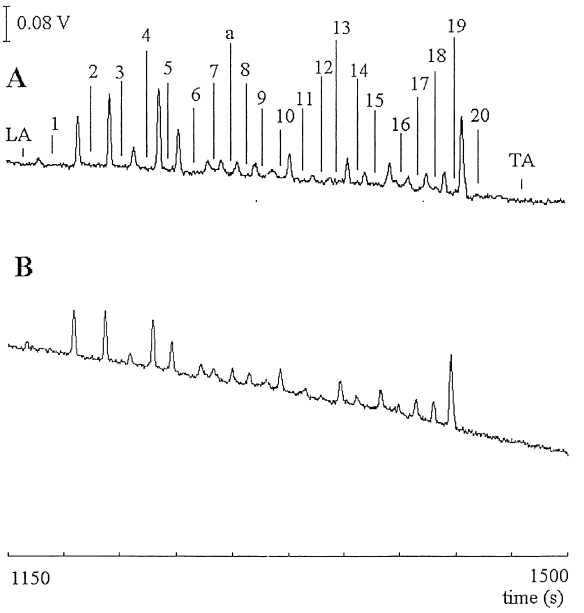

Fig. 4. A long-term repeatability of the blank runs with the discrete spacers. The records were obtained at 405 nm with different lots of the leading and terminating electrolyte solutions (Table 1). 30 μl volumes of the solutions of the discrete spacers (Table 2) were injected by the sample loop of the injection valve. The spacers in the injected samples were at 50 μmol/l concentrations. The meaning of the symbols is the same as in Fig. 2. For the driving currents see Fig. 1.

4. Conclusions

Our results show that the spike mode of the ITP analysis with a multicomponent mixture of discrete

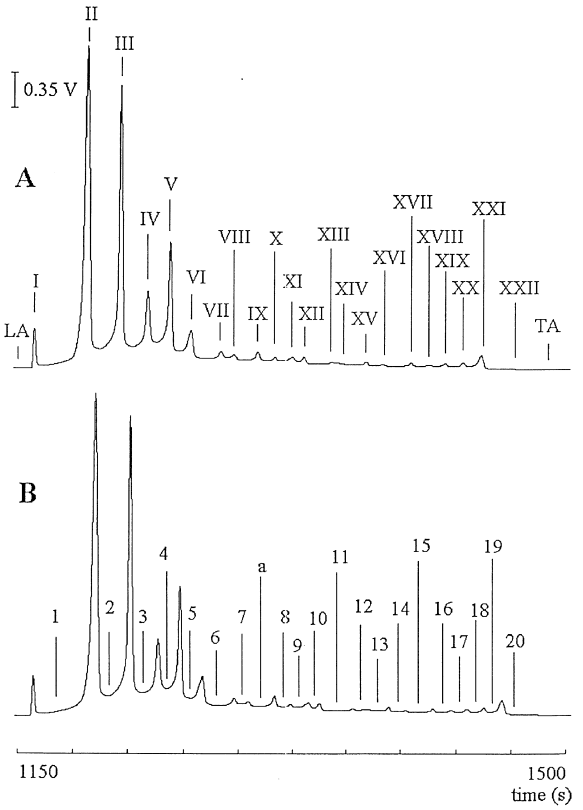

Fig. 5. A repeatability of the isotachophoretic profile of the HA preparation as attained by the photometric detection in the presence of discrete spacers. The records of the profiles were obtained with different lots of the leading and terminating electrolyte solutions and discrete spacers. The injected sample contained in both instances 800 ng of the HA preparation taken from the same stock solution. The concentrations of the discrete spacers (Table 2) were 50 μmol/l. The meaning of the symbols is the same as in Fig. 2. For the driving currents see Fig. 1. LA, TA = leading and terminating anions, respectively.

spacers and with a selective photometric detection operating at a 405 nm detection wavelength offers a promising analytical approach for characterizations of HS samples. From the light absorbing properties of HAs [1–6] one can deduce that a further improvement of the present ITP procedure can be expected by using a multiwavelength photometric detection. Here, diode array detection [46] or dual-wavelength photometric detectors [47] (operating, e.g., at 465 and 665 nm to assess the E_4/E_6 ratio of a particular ITP fraction [1]) are detection alternatives offering more effective use of the ITP separation in the

Table 3
Repeatabilities of the total peak area of the HA constituents and peak areas of the HA fractions distributed along the ITP stack at 405 nm

Fraction No.	Average peak area (mVs)	RSD (%)	Relative size (%)
I	1117	4.1	2.0
II	15557	2.1	27.4
III	12607	2.8	22.2
IV	5163	3.5	9.1
V	6492	3.3	11.4
VI	3296	3.6	5.8
VII	1799	4.0	3.2
VIII	1257	4.3	2.2
IX	1236	4.4	2.2
X	840	5.8	1.5
XI	1108	4.1	2.0
XII	978	4.4	1.7
XIII	715	5.9	1.3
XIV	638	6.2	1.1
XV	579	6.8	1.0
XVI	577	5.4	1.0
XVII	528	7.5	0.9
XVIII	463	7.2	0.8
XIX	474	8.4	0.8
XX	431	8.8	0.8
XXI	723	5.9	1.3
XXII	156	12.1	0.3
Total[a]	56734	2.6	100

[a] 800 ng of the HA preparation loaded into the ITP equipment, the numbers correspond to those to those on isotachopherograms in Figs. 2–5. The data were obtained from five repeated runs.

photometric characterization of the HA fractions. Additional information can be gained by exploiting fluorescence properties of HSs, e.g., in the way as described recently in the CZE separations [17].

Reproducible profiles of the HA constituents in the ITP stack of discrete spacers make the studied approach, for example, promising for a fingerprinting of HSs as obtained in the soil extracts. A further research along this line, in conjunction with a fractionation procedure recently described in the literature [8], is planned in this laboratory.

A twenty-component mixture of discrete spacers as used in this work was undoubtedly ineffective in obtaining pure HA constituents. Although mixtures containing larger numbers of the separable discrete spacers can be probably found there is a limit concerning the number of constituents which can be resolved by ITP in one separation run [48]. This

limit, in fact, sets practical boundaries of the present approach in the ITP characterization of HSs.

Acknowledgements

This work was supported by a grant from the Slovak Grant Agency for Science under the project No. 1/7247/20.

References

[1] M. Schnitzer, Soil Sci. 151 (1991) 41.
[2] E.M. Thurman, R.L. Malcolm, in: R.F. Christman, E.T. Gjessing (Eds.), Aquatic and Terrestrial Humic Materials, Ann Arbor Sci. Publ, Ann Arbor, MI, 1983, p. 1.
[3] M. Schnitzer, in: M. Schnitzer, S.U. Khan (Eds.), Soil Organic Matter, Elsevier, Amsterdam, 1978, p. 1064.
[4] M. Schnitzer, S.U. Khan, Humic Substances in the Environment, Marcel Dekker, New York, 1972.
[5] F.J. Stevenson, Humus Chemistry, Wiley, New York, 1982.
[6] M. Schnitzer, in: R.G. Burns, G. Dell'Agnola, S. Miele, S. Nardi, G. Savoini, M. Schnitzer, P. Segui, D. Vaughan, S.A. Visser (Eds.), Humic Substances: Effects On Soil and Plant, Reda, Milan, 1986, p. 14.
[7] S. Kuwatsuka, A. Watanabe, K. Itoh, S. Arai, Soil Sci. Plant Nutr. 38 (1992) 23.
[8] J. Kandráč, M. Hutta, M. Foltin, J. Radioanal. Nucl. Chem. 208 (1996) 577.
[9] P. Kopáček, D. Kaniansky, J. Hejzlar, Capillary Isotachophoresis of Humic Substances, in: B.J. Radola (Ed.), Electrophoresis Forum 89, Technical University of Munich, Munich, 1989, p. 559.
[10] P. Kopáček, D. Kaniansky, J. Hejzlar, J. Chromatogr. 545 (1991) 461.
[11] A. Rigol, J.F. López-Sánchez, G. Rauret, J. Chromatogr. A 664 (1994) 301.
[12] A. Rigol, M. Vidal, G. Rauret, J. Radioanal. Nucl. Chem. 208 (1996) 617.
[13] A.W. Garrison, P. Schmitt, A. Kettrup, Water Res. 29 (1995) 2149.
[14] S. Pompe, K.-H. Heise, H. Nitsche, J. Chromatogr. A 723 (1996) 215.
[15] P. Schmitt, A. Kettrup, D. Freitag, A.W. Garrison, Fresenius J. Anal. Chem. 354 (1996) 915.
[16] M. Nordén, E. Dabek-Zlotorzynska, J. Chromatogr. A 739 (1996) 421.
[17] M. Nordén, E. Dabek-Zlotorzynska, Electrophoresis 18 (1997) 292.
[18] R. Dunkelog, H.-H. Ruttinger, K. Peisker, J. Chromatogr. A 777 (1997) 355.
[19] A. Rigol, M. Vidal, G. Rauret, J. Chromatogr. A 807 (1998) 275.
[20] U. Keuth, A. Leinenbach, H.P. Beck, H. Wagner, Electrophoresis 19 (1998) 1091.
[21] P. Schmitt-Kopplin, N. Hertkorn, A.W. Garrison, D. Freitag, A. Kettrup, Anal. Chem. 70 (1998) 3798.
[22] P. Schmitt, A.W. Garrison, D. Freitag, A. Kettrup, Water Res. 31 (1997) 2037.
[23] T. Suzuki, H. Hoshino, T. Yotsuyanagi, Bunseki Kagaki 46 (1997) 477.
[24] A. Rigol, J.F. López-Sánchez, G. Rauret, Quim. Anal. (Barcelona) 13 (1994) 11.
[25] A. Gottlein, Eur. J. Soil Sci. 49 (1998) 107.
[26] D. Fetsch, M. Hradilová, E.M. Peña Méndez, J. Havel, J. Chromatogr. A 817 (1998) 313.
[27] D. Fetsch, M. Fetsch, E.M. Peña Méndez, J. Havel, Electrophoresis 19 (1998) 2465.
[28] B.L. Sharp, J. Batey, I.S. Begley, D. Gregson, J. Skilling, A.B. Sulaiman, G. Verbogt, J. Anal. Atom. Spectrom. 14 (1999) 99.
[29] P. Schmitt-Kopplin, A.W. Garrison, E.M. Perdue, D. Freitag, A. Kettrup, J. Chromatogr. A 807 (1998) 101.
[30] D. Fetsch, J. Havel, J. Chromatogr. A 802 (1998) 189.
[31] H.J. Issaq, Electrophoresis 18 (1997) 2438.
[32] D.H. Craston, M. Saeed, J. Chromatogr. A 827 (1998) 1.
[33] D. Fetsch, A.M. Albrecht-Gary, E.M. Peña Méndez, J. Havel, Scripta Fac. Sci. Nat. Univ. Masaryk Brun. Chem. 27–28 (1998) 3.
[34] J. Dahlen, S. Bertilsson, C. Pettersson, Swed. Environ. Int. 22 (1996) 501.
[35] M. De Nobili, G. Bragato, A. Mori, J. Chromatogr. A 863 (1999) 195.
[36] D. Tonelli, R. Seeber, C. Ciavatta, C. Gessa, Fresenius J. Anal. Chem. 359 (1997) 555.
[37] F.M. Everaerts, J.L. Beckers, Th.P.E.M. Verheggen, Isotachophoresis, Elsevier, Amsterdam, 1976.
[38] P. Boček, M. Deml, P. Gebauer, V. Dolník, Analytical Isotachophoresis, VCH, Weinheim, 1988.
[39] P. Gebauer, P. Boček, M. Deml, J. Janák, J. Chromatogr. 199 (1980) 81.
[40] L. Arlinger, J. Chromatogr. 91 (1974) 785.
[41] M. Svoboda, J. Vacík, J. Chromatogr. 119 (1976) 539.
[42] D. Kaniansky, V. Madajová, J. Marák, E. Šimuničová, I. Zelenský, V. Zelenská, J. Chromatogr. 390 (1987) 51.
[43] D. Kaniansky, J. Marák, P. Rajec, A. Švec, M. Koval', M. Lúčka, G. Sabanoš, J. Chromatogr. 470 (1989) 139.
[44] V. Jakúbek, M.Sc. Thesis, Comenius University, Bratislava, 1992.
[45] J. Marák, J. Laštinec, D. Kaniansky, V. Madajová, J. Chromatogr. 509 (1990) 287.
[46] M. Goto, K. Irino, D. Ishii, J. Chromatogr. 346 (1985) 167.
[47] J.C. Reijenga, Th.P.E.M. Verheggen, F.M. Everaerts, J. Chromatogr. 267 (1983) 75.
[48] E. Kenndler, Anal. Chim. Acta 173 (1985) 139.
[49] T. Hirokawa, M. Nishino, N. Aoki, Y. Kiso, Y. Sawamoto, T. Yagi, J. Akiyama, J. Chromatogr. 271 (1983) D1.
[50] T. Hirokawa, T. Gojo, Y. Kiso, J. Chromatogr. 369 (1986) 59.

[51] T. Hirokawa, T. Gojo, Y. Kiso, J. Chromatogr. 390 (1987) 201.
[52] J. Pospíchal, M. Deml, P. Boček, Chem. Rev. 89 (1989) 419.
[53] Biochemical Organic Compounds For Research and Diagnostic Reagents, Sigma, St. Louis, MO, 1991.
[54] S. Kotrlý, L. Šucha, Handbook of Chemical Equilibria in Analytical Chemistry, Ellis Horwood, Chichester, 1985.
[55] D.A. Bender, Amino Acid Metabolism, Wiley, London, 1975.